

ON THE MULTIFRACTAL CHARACTERIZATION OF SPATIAL DISTRIBUTIONS OF AMEDAS RAINFALL

Assela PATHIRANA¹, Srikantha HEARTH¹ and Katumi MUSIAKE¹

¹Institute of Industrial Science, University of Tokyo,
4-6-1, Komaba, Meguro-Ku, Tokyo 153-8505, JAPAN

Multifractal analysis was performed on hourly spatial rainfall for Kanto region, from two sources, namely, interpolated rain gauge data and radar estimated rainfall grids. An attempt was made to make the data sets for analysis from the two sources as similar as possible by selecting same, spatial extent, spatial resolution and record precision. It was found out that in both cases, a single multifractal model can explain all the scales involved in the analysis, from 0.1^0 to 0.8^0 . Multifractal parameters derived for a hundred high rainfall events of a year showed that, for these high rainfall events, the parameter C_1 is agreeing quite close in two data sources, while the Lévy index, α shows a significant scatter. We suggest that even with distributions, which are apparently similar, scaling properties can show significant differences. Finally we give a qualitative explanation for the marked difference of scatter in the relationship for different multifractal parameters by comparing with the relationships of the ‘traditional’ statistics like grid mean, maximum rainfalls and wet fractions for the two data sources.

Key Words: *Multifractals, Scaling, Spatial Rainfall, Radar Precipitation*

1. INTRODUCTION

Until very recent times, there was no reliable method to measure rainfall in space. Rain gauge networks are often too sparse to capture the spatial variations in small scales properly. Recent innovations in Radar estimation of rainfall have provided an alternative means of studying spatial variation in a more continuous manner. While on one hand the radar estimates give more spatially continuous measurements that facilitate spatial analysis, on the other hand caution should be practiced in using those, since radars do not measure rainfall directly as rain gauges do.

In the recent literature there are a number of reports on multifractal characterization of spatial rainfall estimated by gauge data interpolation¹⁾ and by radar estimates²⁾. Most of these attempts have concentrated on one particular method of spatial rainfall estimation. AMEDAS rainfall measuring network of Japan Meteorological Agency, having both an extensive and dense point scale measurement network as well as calibrated country-wide radar estimations³⁾, provides a unique opportunity to compare the per-

formance of said two methods in terms of scaling properties.

In this manuscript we present the results of multifractal analysis of radar derived and gauge derived rainfall estimates in spatial scale. Rain gauge network data, originally in point scale values were interpolated to provide spatial rainfall maps. Radar rainfall maps were extracted from the countrywide compiled radar grid rainfalls. After processing the two types of data to have same spatial resolution and record precision, multifractal analysis was performed. The primary objective of this analysis was to compare various multifractal parameters estimated from two data sources. Finally the parameter deviations are explained in terms of the comparisons of the ‘traditional’ statistics of two data sources.

2. THEORY

Under fairly general conditions, the properties of a random variable, $P(R \geq r)$, that describes a intensity distribution of a measure, R , can be equivalently described by all the statistical moments, $M(q)$ of the distribution defined below:

$$M(q) = \langle R^q \rangle \quad \forall q. \quad (1)$$

For small values of q , $M(q)$ comprises mainly of moments contributing from small (and frequent) values, while the large values of q results in moments where the major contribution is from extreme (and infrequent) values. We express the statistical moment at a given intensity by a scaling exponent $K(q)$ as⁴⁾

$$\langle R^q \rangle \sim \lambda^{K(q)} \quad (2)$$

where $\lambda = L/l$; l is the scale of interest and L is a largest scale involved (an arbitrary value). For spatial analysis l and L are measured in length units. The notation $\langle \rangle$ is used to denote ensemble (climatological) average, though in usual practice it is taken as arithmetic mean.

For multifractal fields that are scaling (i.e. there is a similarity between measurements of various scales) the function $K(q)$ is unique for all scales and can be expressed as⁵⁾

$$K(q) = \begin{cases} \frac{C_1}{\alpha-1}(q^\alpha - q), & 0 \leq \alpha < 1, \quad 1 < \alpha \leq 2 \\ C_1 q \log(q), & \alpha = 1 \end{cases} \quad (3)$$

where C_1 and α (known as Lévy index) are constants. For scaling fields the condition $0 \leq \alpha \leq 2$ should be met with. The parameters C_1 and α describe a scaling field in a range of scales.

(1) Double Trace Moment (DTM) Analysis Technique

DTM analysis is a technique developed by Lavallée (1991)⁶⁾ to determine the multifractal model parameters based on generalized moments. The application of the method is straightforward: First, the original field is raised in to a power η at the smallest scale (λ'). Then the field is aggregated to the needed scale, λ and raised to the usual exponent q . The resulting ‘double’ moment can be assumed to have a scale relationship of the following form.

$$\langle (R_{\lambda'}^\eta)_{\lambda}^q \rangle \sim \lambda^{K(q,\eta)} \quad (4)$$

The resulting exponent $K(q,\eta)$ can be related to the usual exponent $K(q)$ as:

$$K(q,\eta) = \eta^\alpha K(q) \quad (5)$$

which allows the determination of α as the slope of the linear part of the plot of $K(q,\eta)$ against η in logarithmic scale. By considering

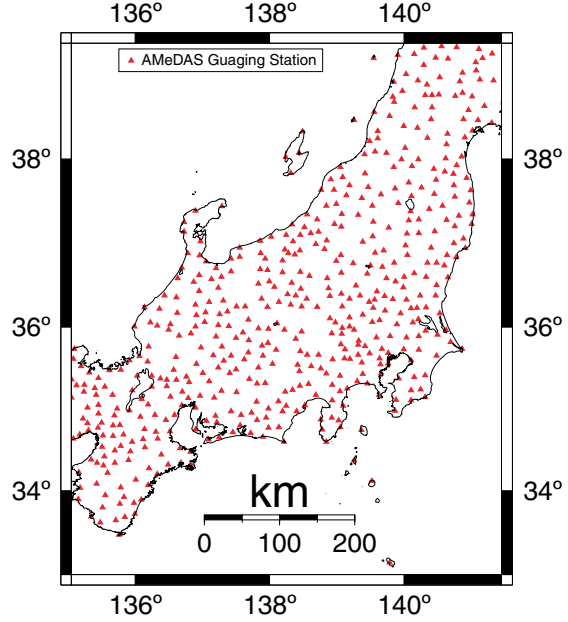


Fig. 1 Location of AMeDAS rain gauges in the selected area

$K(q,1) = K(q)$, C_1 can be determined from equation 3 by the intercept of that linear part. Since, the calculation can be repeated for a range of values of q it is possible to obtain a statistical estimation for multifractal parameters.

3. DATA

(1) Gauge Rainfall

The analysis was limited to the Kanto region of Japan, in order to have a reasonably climatologically homogeneous area. In the selected region there are about 510 rain gauging stations (Figure 1). The rainguage data was interpolated using Thiessen polygon method. Preliminary analysis showed that, with the present rain gauge density the finest spatial resolution that can reasonably retain spatial variations is 0.1° and thus it was selected as the grid cell size for the rainfall grids. All the grids that are not closer than 20km to any of the rain gauges were removed from the analysis, since the precipitation at such grids is likely to be much off from the value observed at the nearest gauging station, though the interpolation method assigns the value of the nearest gauging station.

The resulting dataset of each time period is similar to that shown in figure 2. Before proceeding to multifractal analysis there is one additional step to be performed. The mathematical theory of multifractals (in two dimension) that

was used in this manuscript was developed for rectangular part of the multifractal field, with no missing values. Then the number of boxes $N(l)$ with side l contained in the region follows the relationship $N(l) = l^{-D}$ where $D = 2$. (In fact D is known as the *Hausdorff-Besicovitch dimension* or the *fractal dimension*, and can take non-integer values for complex shapes.) It is fairly straightforward to apply the analysis to a field with missing value. The only change in computation is that when making ensemble averages of moments, the missing values should be ignored. However when the ‘non-missing’ area is of a very irregular shape as shown in figure 2, the exponent D in the relationship of the (computable) number of boxes become different from 2 (the *topological dimension* for 2-dimensional space). This induces an error in the moment computations and should be avoided.

The rainfall grid was divided to $0.8^0 \times 0.8^0$ boxes and each box that has a large number of missing values was eliminated from the grid. The resulting grid shown in figure 3 maintains (above discussed) $D = 2$ from the smallest grid size (0.1^0) to 0.8^0 . Thus, by limiting the analysis to scales below 0.8^0 , we can effectively get rid of the grid irregularity effect.

(2) Radar Rainfall

The preparation of radar rainfall grids is straightforward. From the radar AMeDAS product, the hourly radar maps were extracted for the area of interest. There is an important difference between the radar grid products used in the analysis and the prepared gauge based grids. While the grids prepared from rain gauge data has $0.1^0 \times 0.1^0$ size, the radar grids are of $0.0625^0 \times 0.05^0$ size, which gives the latter a nearly square shape in the latitudes near Japan. Figure 4 shows the radar rainfall grid for the same hour as figures 2 and 3.

In order to minimize comparison errors, the radar rainfall grids were also resampled (using bilinear interpolation as described by Wessal and Smith⁷⁾) to create grids of $0.1^0 \times 0.1^0$ size. Then the data outside the ‘effective area’ of the gauge derived rainfall (explained in section (1) and figure 3) was removed to eliminate possible errors due to spatial-inhomogeneity. Finally, the registrations less than $1mm$ were removed (replaced by zero), as the minimum precision of rain gauge data was $1mm$. Figure 5 shows the final radar grid used for the analysis.

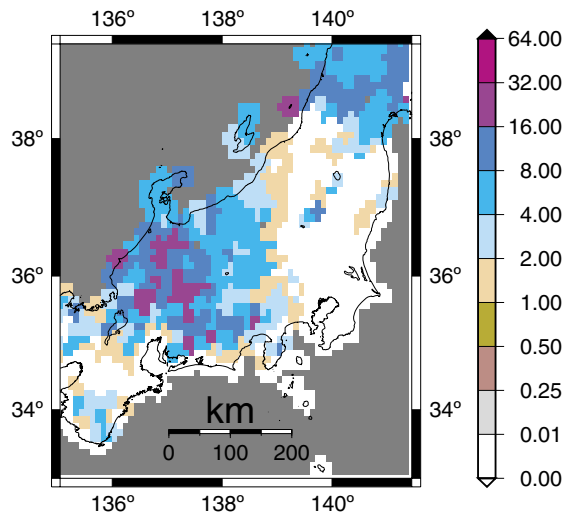


Fig. 2 An example of the rainfall grids created by interpolating rain gauge data. Date: 1997/Jun/28 21:00hrs.

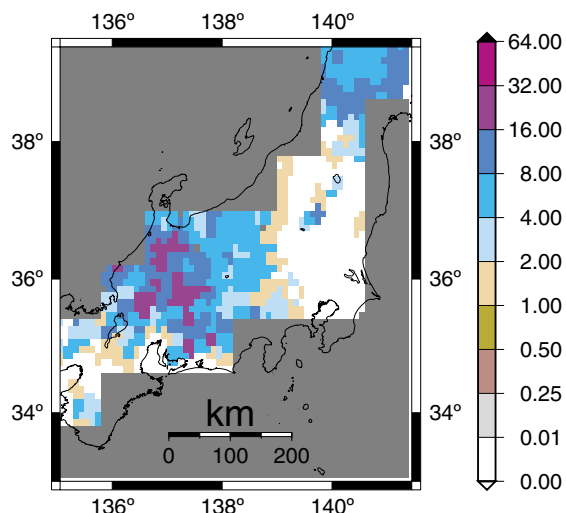


Fig. 3 Final set of gauge-derived grids available for analysis, after removing partially filled $.8^0 \times .8^0$ boxes. Date: 1997/Jun/28 21:00hrs.

4. ANALYSIS

A usual first step in multifractal analysis is to normalize the data to have mean of unity. After normalizing the procedure of analysis is as follows: For a given q , $\langle (R_\lambda^\eta)^q \rangle$ (DTM value) is calculated for a range of values of η . This is done by raising the observed values to power of each η at the highest resolution ($0.1^0 \times 0.1^0$ for gauge interpolated grids, $0.0625^0 \times 0.05^0$ for radar data). Then the grid values are computed at each resolution (e.g. original resolution, 2×2 of original resolution, 4×4 of original resolution and so on).

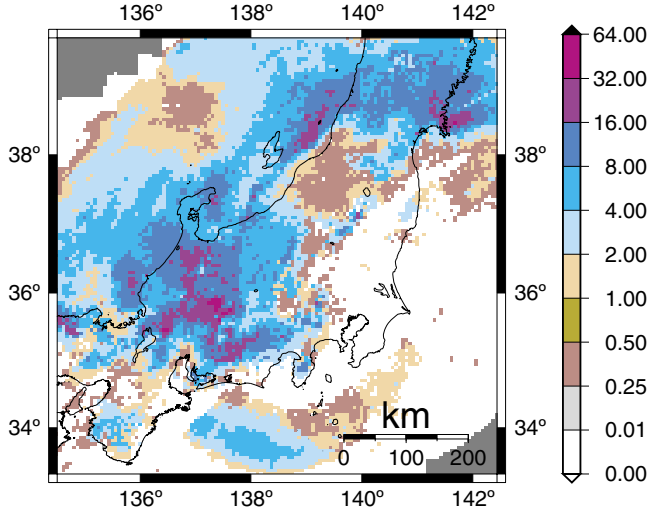


Fig. 4 A radar rainfall grid used for the analysis. An area larger than that is used for the analysis is shown here. Date: 1997/Jun/28 21:00hrs.

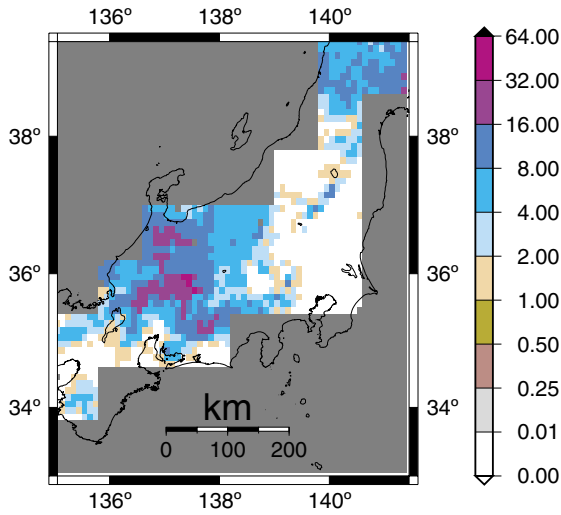


Fig. 5 A radar dataset ready for comparison with gauge derived data. Date: 1997/Jun/28 21:00hrs.

λ value for each resolution is computed as the ratio of that scale to the largest available scale (e.g. we consider the largest scale for radar data as 128x128 grids, so for the case of 2x2 grids, $\lambda = 128/2$). The DTM value is plotted against λ in logarithmic scale. Figure 6 shows such a graph for $q = 1.4$. The linearity of the curves show that the whole range of scales involved can be explained by a single scaling model.

Finally the estimated $K(\eta, q)$ values are plotted against η in logarithmic scale. Figure 7 shows such a graph for some selected values of q . The multifractal parameters α and C_1 can be esti-

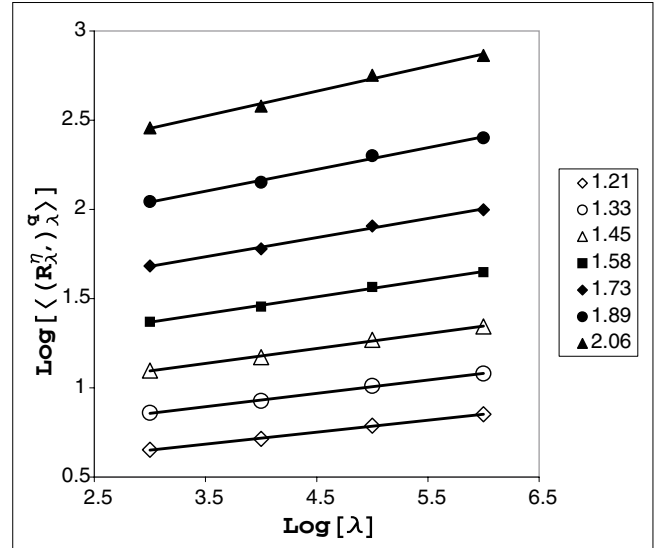


Fig. 6 Plot of $\langle (R_\lambda^q) / \lambda^q \rangle$ (DTM) against λ for $q = 1.4$. Logarithms are calculated to base 2. Date: 1997/Jun/28 21:00hrs.

mated from this plot as explained earlier.

5. RESULTS

Results for hundred rainfall hours in the year 1997 with more than 90% radar coverage of the initial radar grids, and with largest average rainfall values in final gauge-based grids were analyzed.

(1) rainfall comparison

Figure 8 shows the scattergram of mean rainfall for the selected hundred stations. It seems that for these high rainfall events, the grid average rainfall is in good agreement between radar and gauge based estimations. The comparison of maximum grid values are shown in figure 9. While the agreement between two estimates is generally close, the radar-based estimations seem to be higher by an approximately fixed amount of 6 ± 7 mm. Further the scatter in this comparison is substantially larger than that of the comparison of the means. The comparison of the fraction of rainy cells in each grid (Figure 10) shows that the values for radar estimations are generally less than those of gauge estimations.

(2) Fractal Parameters

Figures 11 and 12 show the comparison of multifractal parameters C_1 and α respectively. While there is a very close agreement between C_1 values estimated by two methods, α values show a larger difference as well as a scatter from the av-

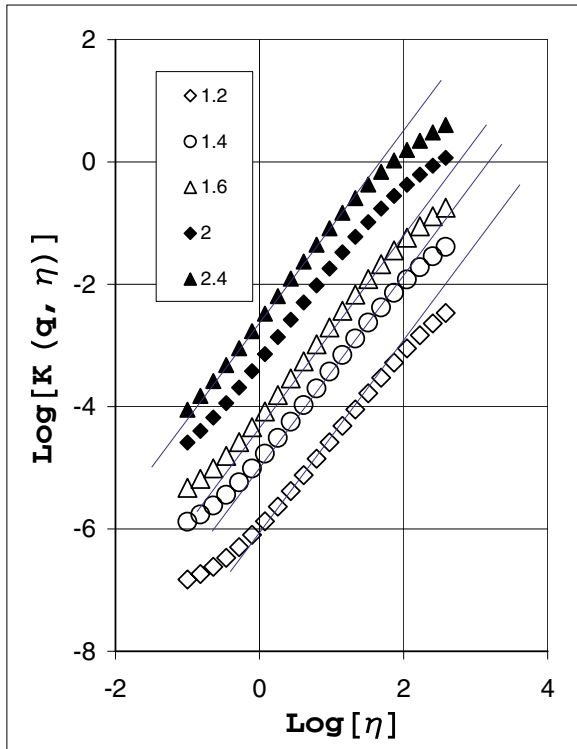


Fig. 7 Plot of $K(q, \eta)$ against η for some selected values of q . Logarithms are calculated to base 2. Date: 1997/Jun/28 21:00hrs.

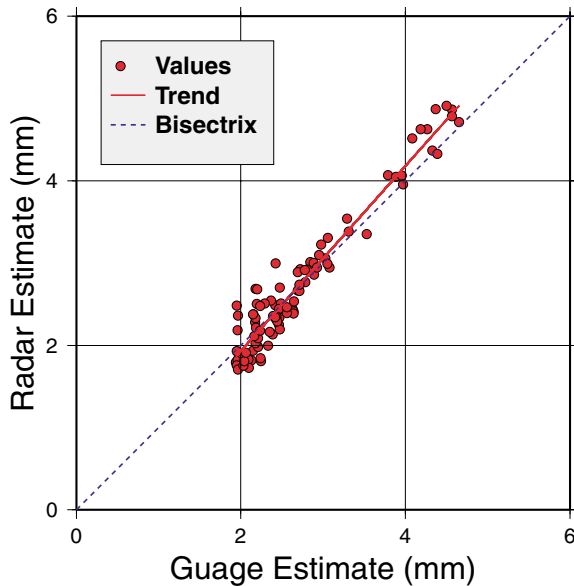


Fig. 8 Comparison of grid-mean rainfall values.

erage relationship.

6. DISCUSSION

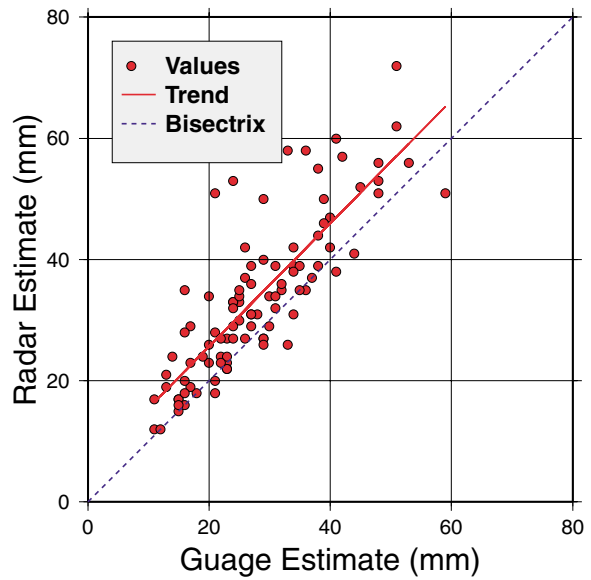


Fig. 9 Comparison of maximum rainfall values.

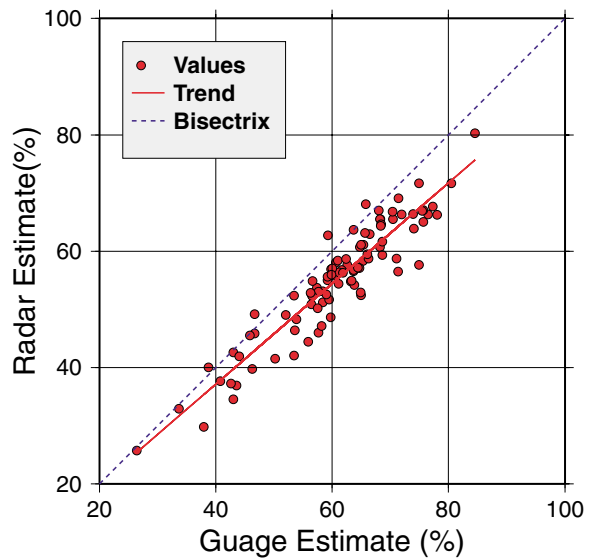


Fig. 10 Comparison of wet fraction in grids.

(1) Multifractality in Space

The analysis presented shows that the multifractal model can be used to understand the spatial distribution of rainfall. Within the (small) range of scales of cell size of 0.1^0 to 0.8^0 the scaling behavior was established. The physical limits of scaling regime in spatial scale can not be estimated due to the fact that analysis outside this resolution limit (from $0.1^0 \times 0.1^0$ to $0.8^0 \times 0.8^0$ is not possible with the present data configuration.

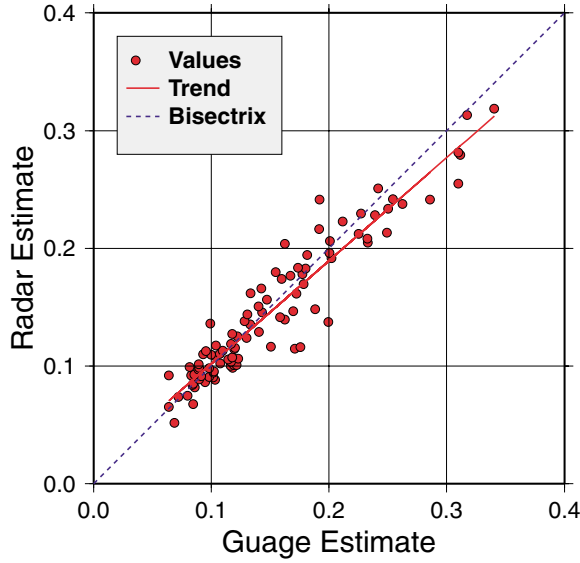


Fig. 11 Comparison of C_1 values.

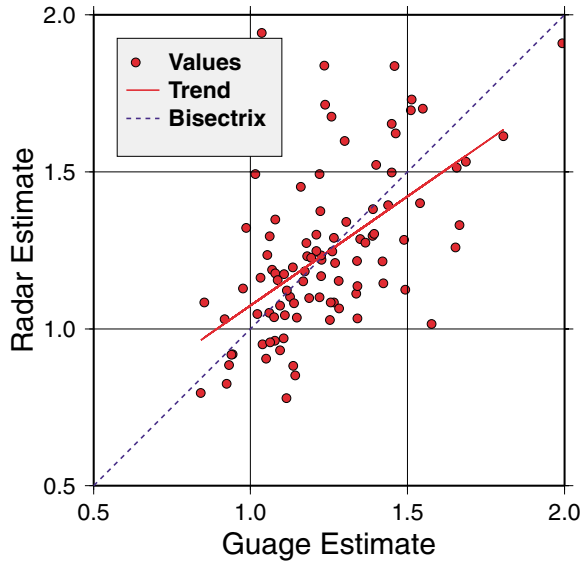


Fig. 12 Comparison of α values.

(2) Parameter relationships

To understand the significance of the difference of multifractal parameters in two types of data, the following expression, which is equivalent to equations 2 and 3, is presented⁸⁾:

$$P(\phi_\lambda \geq \lambda^\gamma) \sim \lambda^{-c(\gamma)} \quad (6)$$

$$c(\gamma) = \begin{cases} C_1 \left(\frac{\gamma}{C_1 \alpha} + \frac{1}{\alpha} \right)^\alpha & \alpha \neq 1 \\ C_1 \exp \left(\frac{\gamma}{C_1} - 1 \right) & \alpha = 1 \end{cases} \quad (7)$$

(for $0 \leq \alpha \leq 2$)

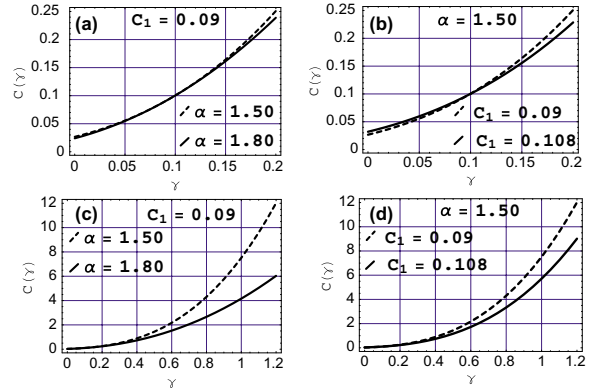


Fig. 13 Sensitivity of $c(\gamma)$ function to the changes in multifractal parameters C_1 and α . (a) and (c): Sensitivity of α ; (b) and (d): sensitivity of C_1 .

where γ is a constant. Here the functions $K(q)$ and $c(\gamma)$ are related by a Legendre transform⁹⁾:

$$\begin{aligned} c(\gamma) &= \max_q (q\gamma - K(q)) \\ K(q) &= \max_\gamma (q\gamma - c(\gamma)) \end{aligned} \quad (8)$$

$c(\gamma)$ which is a function of C_1 and α is directly related to the exceedance probability of values of the field. Thus, the relationship of the multifractal parameters, C_1 and α and the values in the multifractal field can be better understood by examining effect of those parameters on the value of $c(\gamma)$ function. Figure 13 shows plots of $c(\gamma)$ function for two ranges of γ . Graphs on top covers values of γ from 0 to .2. These represent the grid values from the mean to 2-3 times of the mean in the normalized grid values. Graphs on the bottom covers values up to about 150 times the mean value. Two points are made clear from these graphs: 1) The sensitivity of $c(\gamma)$ function (i.e. sensitivity of exceedance probability, P) to α is largely limited to the high values of $c(\gamma)$ (i.e. extreme values). 2) The sensitivity of C_1 is present both for extreme values and 'normal' values.

These observations provide important clues as to why the α parameter shows a significant scatter between radar and gauge estimates while C_1 shows very much less scatter. The scatter of the mean rainfall (Figure 8) and that of fraction of wet cells (Figure 10) show significantly low scatter compared to the maximum grid value (Figure 9). (One reason for this difference may be the large sample size involved in mean and wet fraction calculations.) One of the features of multiscaling models is that they are quite sensitive to extreme values. As explained before, this sensi-

tivity in the current model is mainly with the parameter α (Figure 13). Hence it is usual for the two estimates of α values to show more scatter than those for C_1 values.

7. CONCLUSIONS

Using radar data for multifractal analysis of spatial rainfall is an appealing alternative to interpolation of gauge data due to many reasons. In this study we found that while it is true that the spatial patterns from two methods behave in a very similar patterns, there are some points that demands closer attention.

Overall statistics of radar and gauge interpolated rainfall agree well. However, in the case of multifractal analysis, only C_1 values are agreeing closely while the estimations of α shows a significant scatter. We try to explain this behavior with the fact that in the multifractal model adopted, the value of α is related largely with extreme values of the distribution, while C_1 relates to ‘normal’ values as well as (to some extent) to the extreme values. α ’s ‘sole’ dependence on extreme values seen together with significant scatter of maximum values in radar and gauge comparison explains the relatively poor relationship of α in the comparison.

ACKNOWLEDGMENT: We thank J. Olsson of Institute of Environmental Systems (SUIKO) of Kyushu University, Fukuoka, formerly of Lund University, Sweden, for his guidance on multifractal analysis.

REFERENCES

- 1) J. Olsson and J. Niemczynowicz, Multifractal analysis of daily spatial rainfall distributions, *Journal of Hydrology*, 187 29-43, 1996.
- 2) R. Deidda, Rainfall downscaling in a space-time multifractal framework, *Water Resources Research*, 36 7 1779-1794, 2000
- 3) Y. Makihara, A method for improving radar estimates of precipitation by comparing data from radars and rain gauges, *Journal of the Meteorological Society of Japan*, 74 459-480, 1996
- 4) D. Schertzer and S. Lovejoy, Physical modelling and analysis of rain and clouds by anisotropic scaling multiplicative processes, *Journal of Geophysical Research*, 92 9693-9714, 1987
- 5) S. Lovejoy and D. Schertzer, Multifractals, universality classes and satellite and radar measurements of clouds and rain fields, *Journal of Geophysical Research*, 95 2021-2034, 1990
- 6) D. Lavallée, Multifractal analysis and simulation technique and turbulent fields Ph.D. Thesis, McGill University, Montréal, Canada 1991, 133pp.
- 7) P. Wessel and W. H. F. Smith, New, improved version of Generic Mapping Tools released, *EOS trans. American Geophysical Union*, 79, 579, 1998.
- 8) Y. Tessier, S. Lovejoy and D. Schertzer, Universal Multifractals: theory and observations for rain and clouds, *Journal of Applied Meteorology*, 2 223-250, 1993
- 9) G. Parisi and U. Frisch, A multifractal model of intermittency, in *Turbulence and Predictability in Geophysical Fluid Dynamics and Climate Dynamics*, edited by M. Ghil, R. Benzi and G. Parisi, North Holland, New-York, 1985, 84-88